ADVANCED BIOLOGY
www.advanced-bio.com

3D Human iPSC Blood Vessel Organoids as a Source of Flow-Adaptive Vascular Cells for Creating a Human-Relevant 3D-Scaffold Based Macrovessel Model

*Elana M. Meijer, Suzanne E. Koch, Christian G.M. van Dijk, Renee G.C. Maas, Ihsan Chrifi, Wojciech Szymczyk, Paul J. Besseling, Lisa Pomp, Vera J.C.H. Koomen, Jan Willem Buikema, Carlijn V.C. Bouten, Marianne C. Verhaar, Anthal I.P.M. Smits, and Caroline Cheng**

3D-scaffold based in vitro human tissue models accelerate disease studies and screening of pharmaceutics while improving the clinical translation of findings. Here is reported the use of human induced pluripotent stem cell (hiPSC)-derived vascular organoid cells as a new cell source for the creation of an electrospun polycaprolactone-bisurea (PCL-BU) 3D-scaffold-based, perfused human macrovessel model. A separation protocol is developed to obtain monocultures of organoid-derived endothelial cells (ODECs) and mural cells (ODMCs) from hiPSC vascular organoids. Shear stress responses of ODECs versus HUVECs and barrier function (by trans endothelial electrical resistance) are measured. PCL-BU scaffolds are seeded with ODECs and ODMCs, and tissue organization and flow adaptation are evaluated in a perfused bioreactor system. ODECs and ODMCs harvested from vascular organoids can be cryopreserved and expanded without loss of cell purity and proliferative capacity. ODECs are shear stress responsive and establish a functional barrier that self-restores after the thrombin challenge. Static bioreactor culture of ODECs/ODMCs seeded scaffolds results in a biomimetic vascular bi-layer hierarchy, which is preserved under laminar flow similar to scaffolds seeded with primary vascular cells. HiPSC-derived vascular organoids can be used as a source of functional, flow-adaptive vascular cells for the creation of 3D-scaffold based human macrovascular models.

1. Introduction

Cardiovascular disease (CVD) is a leading cause of death and morbidity with rising prevalence in Western and Westernized countries.[1] One of the principal disease mechanisms of CVD is the adverse, functional, and structural adaptation of the vascular tissue, leading to clinical complications including myocardial infarction, ischemia, stroke and aneurysms.[2] Studies based on human samples and animal experiments have contributed considerably to build our understanding of the pathways and mechanisms that drive pathological adaptation in CVD. Nevertheless, the involvement of multiple dynamic factors in CVD that interact in complex cross-cell type systems, as well as the fact that animal models are limited in their capacity to mimic the full human disease condition on a physiological and biological level,[3–5] considerably restrict the translatability of these findings to the clinic. Similarly, the growing demand for synthetic 3D vascular scaffolds for surgical replacement of diseased arteries in CVD patients,

E. M. Meijer, C. G.M. Dijk, I. Chrifi, P. J. Besseling, M. C. Verhaar, C. Cheng
Department of Nephrology and Hypertension
Division of Internal Medicine and Dermatology
University Medical Center Utrecht
3584CX Utrecht, The Netherlands
E-mail: k.l.cheng-2@umcutrecht.nl

The ORCID identification number(s) for the author(s) of this article can be found under https://doi.org/10.1002/adbi.202200137.

DOI: 10.1002/adbi.202200137

E. M. Meijer, C. G.M. Dijk, I. Chrifi, P. J. Besseling, M. C. Verhaar, C. Cheng
Regenerative Medicine Center Utrecht
University Medical Center Utrecht
3584CT Utrecht, The Netherlands

S. E. Koch, W. Szymczyk, L. Pomp, V. J.C.H. Koomen, C. V.C. Bouten, A. I.P.M. Smits
Department of Biomedical Engineering
Eindhoven University of Technology
5612AZ Eindhoven, The Netherlands

S. E. Koch, C. V.C. Bouten, A. I.P.M. Smits
Institute for Complex Molecular Systems (ICMS)
Eindhoven University of Technology
5612AZ Eindhoven, The Netherlands

increasingly recognizes the value of the optimization of scaffold prototypes in in vitro bioreactor setups before testing the most improved design in animal studies. In particular, for the emerging field of scaffold based in situ tissue engineering, in which the material design is adapted to exploit the regenerative potential of autologous cells in the host's body to stimulate tissue formation, the step of ex vivo evaluation in high complexity bioreactor models could considerably reduce development costs associated with direct animal testing.[6–8] Human focused in vitro vascular models could also aid in reducing the use of animals in research and improve the translational value of findings. Vascular models that combine cells with biomaterial scaffolds in vitro provide valuable simulates of the in vivo condition to study cell behavior in disease and tissue generation, in a controlled manner that allows systematic evaluation of the impact of individual biological and mechanical cues. Although most in vitro models only rely on established 2D culture techniques, the introduction of biomaterials in combination with solution electrospinning (SES) that allows 3D-scaffold designs that mimic the properties of the ECM environment of the vessel wall, may provide improved models that better recapitulate native in situ cell behavior. This, combined with advancement in the fluidics and bioreactor research field may enable perfused culture of 3D-scaffold based vessels and thus the introduction of fluid forces to the models, enabling the study of the role of hemodynamics in driving vascular disease as well as its impact on vascular regeneration.

To increase human relevance, human induced-pluripotent stem cells (hiPSCs) may be used as an autologous cell source for 3D-scaffold based vascular models. HiPSCs bypass the ethical dilemmas surrounding the use of embryonic stem cells and can be differentiated in any specialized cell type including vascular cells,[9,10] while the required dermal fibroblast or peripheral blood mononuclear cells for iPSC reprogramming can be easily sourced from healthy donors or CVD patients. The use of patient derived hiPSC in this setting also opens the door to complex human in vitro modeling of genetic vascular disease and offers a more direct translational alternative to mouse genetic disease models, as well as providing an ex vivo testing platform to adapt scaffold design for any negative impact of mutations on the patient's autologous regenerative capacity in situ. In vitro tissue engineered human vessels (TEHV) such as rolled cell-sheets based constructs in hydrogel,[11] or expanded polytetrafluoroethylene, silicone or polyglycolic acid (PGA) scaffolds seeded with primary vascular cells have already demonstrated the feasibility of these systems in mimicking native cellular responses after exposure to mechanical and biological stimuli in bioreactor systems.[12,13]

R. G.C. Maas, J. W. Buikema
Regenerative Medicine Center Utrecht
Department of Cardiology
University Medical Center Utrecht
3584CX Utrecht, The Netherlands
C. Cheng
Experimental Cardiology
Department of Cardiology
Thoraxcenter Erasmus University Medical Center
3015GD Rotterdam, The Netherlands

Different culture methods for the generation of only iPSC-derived endothelial cells (ECs) or only iPSC-derived mural cells (MCs) have been previously described,[9,10,14–21] with each study reporting a different set of cell qualities and applications. It was previously shown that iPSC-derived ECs could display similar characteristics of primary endothelial cells in terms of morphology, junction formation, barrier function and shear stress response.[22,23] For iPSC derived MCs, differentiation protocols typically generate smooth muscle-like cells that were similar to human aortic vascular smooth muscle cells (VSMCs) in terms of gene expression patterns, morphology, vascular cell marker expression and in vitro functional properties.[21,24] Although iPSC derived vascular cells are now frequently used in 2D culture studies, only a very limited number of studies have tested their application creating hierarchically organized 3D-scaffold based blood vessels.[25–27] More importantly, reports that demonstrate the combined application of both hiPSC-ECs and hiPSC-MCs for the creation of a complex in vitro 3D-scaffold based human perfused blood vessel model, is currently lacking.

Here we aim to investigate the use of vascular cells from hiPSC-derived vascular organoids, as a cell source for the creation of 3D-scaffold based, biomimetic human blood vessel model in a perfused bioreactor system. Based on the protocol published by Wimmer et al., these blood vessel organoids are composed of endothelial cells and mural cells that self-assemble into vascular networks enveloped by a basement membrane. Vascular differentiation from the mesoderm phase takes place in a 3D environment in which the EC and MC lineages can establish during natural interaction between the different cell types, instead of differentiation in cell type specific isolated cultures.[28] Used in our pipeline this eliminates the need for establishing and maintaining two separate hiPSC-differentiation cultures. Pools of hiPSCs vascular organoid derived ECs and VSMCs can be harvested and expanded in traditional 2D culture without reduction in cell survival and proliferation capacity or loss of cell phenotype. The capacity of organoid derived ECs (ODECs) to respond to shear stress and to establish and regulate endothelial barrier function was demonstrated in 2D assays. ODECs and organoid derived mural cells (ODMCs) were capable to grow and form native-like hierarchical vascular tissue in SES polycaprolactone-bisurea (PCL-BU) 3D-vascular scaffolds comparable to human primary vascular cells. ODECs and ODMCs derived human vessels preserved native-like tissue organization in response to hemodynamic exposure when tested in a previously published perfused bioreactor set-up.[29]

2. Experimental Section

2.1. Cell Culture

2.1.1. Derivation and Culture of Human iPSCs

The hiPSCs (SCVI273) used in this study were kindly donated by the Joseph Wu Lab (Stanford Medicine, Department of Medicine and Radiology, Stanford CVI Biobank). Sendai viral reprogramming was used to generate all hiPSC lines from peripheral blood mononuclear cells obtained from individuals who gave informed consent under protocols approved by the

Stanford University Human Subjects Research Institutional Review Board as described previously.[30] The hiPSC were nonenzymatically passaged using 0.5×10^{-3} M EDTA (Invitrogen) every 4 d. HiPSC clumps were passaged in a splitting ratio of 1:13 routinely at 80% confluence. Cells were plated in matrigel-coated 12-well plates and supplemented with E8 medium. Medium was changed every day. To improve cell survival, split ratio reliability and to reduce selective pressure, 1:2000 ROCK inhibitor (Calbiochem) was used in the first 24 h.

2.1.2. Vascular Organoid Differentiation

HiPSCs were harvested using EDTA and subsequently resuspended in differentiation medium (Dulbecco's modified Eagle's culture medium (DMEM): F12, 20% KnockOut Serum (KOSR), 1% Penicillin Streptomycin (PS), Glutamax and nonessential amino acids (NEAA); all Gibco), including 50×10^{-6} M ROCK-inhibitor Y-27632 (Calbiochem). A schematic overview of the differentiation process is displayed in **Figure 1**a. Cells were plated into an ultra-low attachment six-well plate (Corning), in a final concentration of $2*10^5$ cells per well. Cells were incubated on a shaker plate at 37 °C for 2 h to form aggregates and subsequently transferred to hypoxic conditions (5% O_2). Cell aggregates were treated with 13×10^{-6} M GSK-3 inhibitor CHIR99021 (Tocris) on day 3. On day 5, 7 and 9, the aggregates were treated with bone morphogenetic protein 4 (BMP4) (30 ng mL^{-1}; Stemcell Technologies), vascular endothelial growth factor A (VEGF-A) (30 ng mL^{-1}; Peprotech) and fibroblast growth factor 2 (FGF-2) (30 ng mL^{-1}; Miltenyi Biotec) to promote the vascular lineage. On day 11, medium was supplemented with VEGF-A (30 ng mL^{-1}), FGF-2 (30 ng mL^{-1}) and transforming growth factor β (TGFβ)-inhibitor SB43152 (10×10^{-6} M; Stemcell Technologies) to increase the yield of endothelial cells and suppress excessive differentiation into mesenchymal/mural like cells. The aggregates were collected on day 13, embedded in a 3:1 matrigel:collagen mixture (Atelocollagen Bovine Dermis 3 mg mL^{-1}, Bio-connect) and supplemented with differentiation medium containing 15% fetal bovine serum (FBS), VEGF-A (100 ng mL^{-1}) and FGF-2 (100 ng mL^{-1}). Medium was changed every other day. Vascular organoids were collected on day 18 and either disaggregated for further experiments or cultured in a 96-wells round bottom plate without ECM support to stimulate self-assemble into spheroid-shaped vascular organoids.

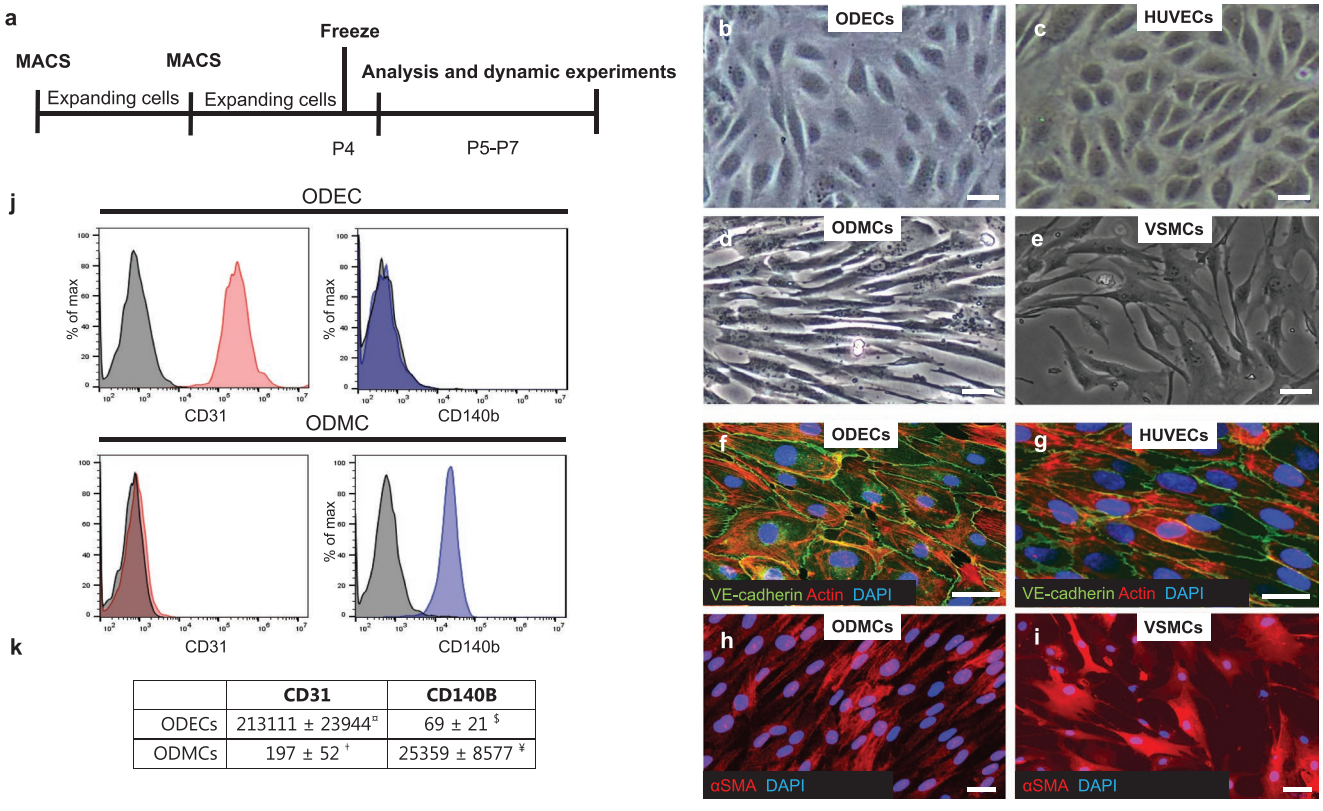

	CD31	CD140B
ODECs	213111 ± 23944[¤]	69 ± 21 [$]
ODMCs	197 ± 52 [†]	25359 ± 8577 [¥]

Figure 1. Validation of ODEC and ODMC populations. a) Schematic overview of the cell culture regime, in which MACS is performed to obtain pure ODEC and ODMC populations. Isolated ODEC and ODMC pools were expanded and stored in liquid nitrogen at P4 prior to further experiments. Validation experiments including FACS analysis were performed after thawing and P5 or P6 cells were used in the dynamic experiments. Bright field pictures of the b) ODECs, c) HUVECs, d) ODMCs, and e) VSMCs. Scale bars represent 20 µm. Immunofluorescent staining of f) ODECs and g) HUVECs for F-actin and EC marker VE-Cadherin and h) ODMCs and i) VSMCs for MC marker αSMA (Smooth muscle Actin). Scale bars represents 20 µm. j) Representative flow cytometry histograms of ODECs and ODMCs stained for both CD31 and CD140b. k) Mean fluorescent intensity (MFI) of ODEC and ODMC. Shown are mean ± SEM, $n = 4$, Paired t-test; [¤] $p < 0.001$ compared to CD140b. [†] $p < 0.05$ compared to CD140b. [$] $p < 0.0001$ compared to ODMCs. [¥] $p < 0.05$ compared to ODECs. P, passage; MACS, magnetic activated cell sorting; ODECs, organoid derived endothelial cells; ODMCs, organoid derived mural cells.

2.1.3. Organoid-Derived Cell Culture

Organoid-derived mural cells (ODMCs) and organoid-derived endothelial cells (ODECs) were labeled P0 directly after sorting (described in section "MACS" below). ODMCs were cultured on SMGM2 medium (Lonza) and ODECs were cultured on EGM2 medium (Lonza) supplemented with TGFβ-inhibitor SB43152 (10×10^{-6} M) and medium was changed every other day. Cells were passaged for expansion using Trypsin/EDTA (Gibco). Cells were harvested at P4 and stored in liquid nitrogen in medium supplemented with 10% FBS and 10% DMSO. Both ODMCs and ODECs were cultured in gelatin coated dishes at 37 °C with 5% CO_2 after thawing and used in experiments till the 7th passage.

2.1.4. Primary Cell Culture

For control experiments, primary human umbilical vein endothelial cells (HUVECs) were purchased from Lonza and maintained in EGM2 medium with 1% PS. Primary human brain-derived vascular pericytes were purchased from ScienCell and maintained in DMEM (Gibco)+10% FBS with 1% PS. Aortic vascular smooth muscle cells (VSMCs) were purchased from Lonza and maintained in SMGM2 medium supplemented with 1% PS. All cell types were cultured till passage 8 in gelatin coated dishes at 37 °C with 5% CO_2.

2.2. Cell Sorting and Analysis

2.2.1. Flow Cytometry

Vascular organoids were mechanically disrupted and disaggregated using 3 U mL^{-1} dispase (Gibco), 2 U mL^{-1} liberase (Roche) and 100 U DNase (Stemcell Technologies) in warm DMEM:F12 for 20 min at 37°C while rotating. To remove excess gel and cell clumps from the suspension, the solution was filtered using a 70 µm cell strainer and spun down for 5 min at 400 g. Cells were subsequently stained with anti-CD31 and anti-CD140b antibodies (Table S1, Supporting Information), together with Sytox blue (Invitrogen) to exclude dead cells. CytoFLEX flow cytometer (Beckman Coulter) was used for cell analysis and data analysis was performed using FlowJo software (Version 10.2).

2.2.2. Magnetic-Activated Cell Sorting (MACS)

Vascular organoids were dissociated as described above. To ensure purity of the populations, cells were separated using a 2-step protocol. The cells were labeled with anti-CD140b antibody (PE) and subsequently with anti-PE magnetic beads. Cell pools were separated using the LS column (Miltenyi Biotec) on the MidiMACS (Miltenyi Biotec) separator according to manufacturer's instructions. Cells positive for CD140b were further cultured in a gelatin-coated six-well plate, supplemented with SMGM2 medium. Cells negative for CD140b were stained with anti-CD31 magnetic beads and cell pools were separated using the LS column on the MidiMACS separator again. Cells positive for CD31 were further cultured on a gelatin-coated six-well plate, supplemented with EGM2 medium. Single-step MACS protocol was performed after 2 passages, to ensure purity of the populations. Anti-CD31 labeling was used for ODECs and anti-CD140b was used for ODMCs.

2.2.3. Quantitative Polymerase Chain Reaction Analysis

Total RNA was isolated from cultures (ODECs, ODMCs, HUVECs, Pericytes and VSMCs) using RNA isolation kit (Bioline) according to the manufacturer's instructions. RNA from organoids and TEVGs was isolated using Trizol (Invitrogen) according to manufacturer's instructions. The purity and concentrations of RNA were quantified using spectrophotometry (DS-11; DeNovix) absorbance measurements at 260/280 nm. cDNA synthesis was performed according to the instructions from the Bioline cDNA synthesis kit. Gene expression was determined using FastStart SYBR-green (Roche) following the quantitative polymerase chain reaction (qPCR) program: 8,5′ 95 °C, 38 cycles (15″ 95 °C; 45″ 60 °C) 1′ 95 °C, 1′ 65 °C, 62 cycles (10″ 65 °C + 0.5 °C) in the SYBR-Green-Cycler IQ5 detection protocol (Biorad CFX384), performed in 384-wells plates (Merck). The primer sequences used are listed in Table S2 (Supporting Information). All results were normalized for house-keeping gene β-actin, resulting in relative mRNA expression. In dynamic experiments, results were compared to static controls and represented as fold change ($\Delta\Delta$Ct).

2.3. In Vitro Assays

2.3.1. PrestoBlue Assay

Cells (N = 5 different vials) were seeded on a gelatin coated six-well plate with a cell density of $5*10^4$ cells per well. Cell viability was measured 24, 72 and 120 h post-seeding using PrestoBlue Cell Viability Reagent (ThermoScientific) according to manufacturer's protocol.

2.3.2. PicoGreen Assay

Cells (N = 5 different vials) were seeded on a gelatin coated six-well plate with a cell density of $5*10^4$ cells per well. To quantify the amount of double stranded DNA, a Quant-iT PicoGreen dsDNA Assay (ThermoFisher) was performed 24, 72 and 120 h post-seeding according to manufacturer's protocol.

2.3.3. Transendothelial resistance measurements

ODECs ($9*10^4$, N = 4 individual experiments) and HUVECs ($5*10^4$, N = 3 individual experiments) were seeded on a 0.1% gelatin permeable filter insert (0.4 µm pore, Falcon). Before the experiment, the resistance (Rblank) was measured by placing unseeded inserts in an Endohm-SNAP chamber filled with 5 mL of EGM2 medium (World Precision Instruments).

The chamber was coupled to an EVOMX resistance meter (World Precision Instruments). The transendothelial electrical resistance (TEER) was measured daily to monitor resistance buildup during growth toward full confluence. At day 4, confluent monolayers were treated with 1 U mL^{-1} thrombin (Sigma) for 30 min while the TEER was measured every 5 min. After 30 min, the thrombin solution was washed away and replaced with normal medium. TEER was measured every 15 min during the restoration phase for 2 h.

2.3.4. 2D flow experiments

ECs (N = 4 individual experiments) were seeded on collagen IV (HUVECs) or gelatin (ODECs) coated 6-channel μ-slides (VI 0.4, Ibidi) with a cell density of $1*10^6$ cells mL^{-1}. The ECs were suspended in culture medium (40 µL/channel) and 1% PS. After 1 h incubation (37 °C, 5% CO_2), 100 µL of EGM2 medium was added into each channel. The cells were cultured statically for 24 h before exposure to shear stress. Medium was changed after 24 h for the static control conditions. An overview of the applied incremental shear stress levels can be seen in Table S3 (Supporting Information). For each Ibidi system, the red perfusion set (Ibidi) in combination with a fluidic unit (Ibidi) and flow pump system (Ibidi) was used to create a unidirectional laminar flow. The μ-slides were connected in series. The μ-slides were subjected to wall shear stress for 48 h (1.5 Pa) after which two channels were fixed and used for immunostaining and four channels harvested and pooled for RNA isolation.

2.4. 3D Experiments

2.4.1. Scaffold preparation

Tubular scaffolds (Ø 3 mm, 25 mm, 250 µm wall thickness, isotropic fiber orientation, 5 µm fibers) were produced using electrospinning. The tubular scaffolds were electrospun from 23.3% (w/w) bis-urea (BU)-modified poly(ε-caprolactone) (PCL-BU, SyMO-Chem,) and 76.7% (w/w) chloroform (Sigma) polymer solutions, which were transferred (flow rate: 40 µl/min) through a charged needle (18 kV) toward the negatively charged (-1 kV) rotating mandrel (400 rpm), which was placed at 17.5 cm distance in the climate controlled cabinet (23 °C and 30% relative humidity, IME Technologies). To facilitate scaffold removal, the mandrel was coated prior to electrospinning with 5% (w/v) poly(ethylene oxide) (PEO, Sigma, M_w 900 kDa) aqueous solution. This electrospraying PEO solution was transferred (flow rate: 7.5 µl min^{-1}) through a charged needle (15 kV) toward a negatively charged, rotating 3 mm Ø mandrel (-1 kV, 1000 rpm, needle-mandrel distance: 16.5 cm). After electrospinning, the scaffolds were removed from the mandrels, cut to size (25 mm in length) and placed in a vacuum oven at 37 °C overnight to remove residual solvent.

Before cell seeding, the scaffolds were sterilized by UV-light exposure with wavelength of 253.7 nm (30 min/side), incubated in phosphate buffered saline (PBS) and 2% PS (Lonza) for 24 h and afterward coated in a collagen I/fibronectin solution (30 µg mL^{-1} rat tail collagen I; Corning, 50 µg mL^{-1} fibronectin from bovine plasma; Sigma-Aldrich) for 1 h at 37 °C to enhance cell adhesion and retention to the graft. Thereafter, the scaffolds were incubated in culture medium with 10% FBS for 24 h.

2.4.2. Cell seeding

ODMCs and ODECs were seeded separately to obtain a bilayered structure of the vascular graft (N = 4 individual experiments). Prior to cell seeding, culture medium was removed and $3.8*10^6$ ODMCs/graft were seeded using fibrin as a cell carrier as described before.[31] In short, cells were suspended in a mixture of fibrinogen (bovine, 10 mg mL^{-1}, Sigma) and thrombin (bovine, 10 IU mL^{-1}, Sigma) and homogeneously dripped over both the lumen and adventitial side of the graft. To promote a uniform distribution of cells, the cell-loaded constructs were rotated by 180° every 15 min in a general incubator (37 °C, 5% CO_2) for 1 h. After 1 h polymerization at 37 °C, SMGM2 medium with 0.25 mg mL^{-1} ascorbic acid was added to induce ECM production and ODMCs were further cultured in static conditions for 48 h.

After 48 h, the same procedure was repeated with ODECs ($3.8*10^6$ ODEC's/graft) which were only seeded on the luminal side of the graft. The ODMCs- and ODECs-seeded graft was cultured statically for another 5 d in 1:1 SMGM2 with ascorbic acid and EGM2 media.

2.4.3. Hemodynamic loading of vascular graft

After 7 d of static culture, the grafts were mounted into a previously developed vascular flow bioreactor[29] and connected to the flow loop to start the 48 h perfusion period. The flow bioreactor is designed to allow for culturing of vascular constructs with separated luminal and adventitial media to support vascular co-cultures, as previously described in detail.[29] The seeded tubular grafts were connected to a Luer Lock Connector Male (Ibidi) and a Luer Connector Male (Ibidi) on each side of the graft and mounted in the custom-made culture chamber with surgical prolene sutures (4-0 Ethicon, Johnson&Johnson), connecting the luminal side of the graft to the flow loop for unidirectional flow application, controlled by a flow pump system (Ibidi) with two medium reservoirs with EGM2 medium (total volume 8 mL medium/reservoir). Subsequently, the bioreactor was closed and the outer compartment was filled with SMGM2 medium supplemented with ascorbic acid. The bioreactor was placed in a general incubator (37 °C, 5% CO_2). Gradually increased shear stress was applied toward 0.08 Pa with a flow rate toward 18 mL/min (Table S3, Supporting Information). Static controls were connected to the pump system, and subjected to the minimum amount of flow (0.01 Pa) to allow for medium exchange. An overview of the shear stress levels applied on the TEVG, can be seen in Table S3 (Supporting Information). Grafts seeded with HUVECs and VSMCs were used as control, and coupled to the same flow pump in parallel to the organoid seeded grafts.

2.4.4. Scanning Electron Microscopy

The microstructure and surface coverage of the electrospun PCL-BU graft was analyzed using scanning electron microscopy (SEM) (Quanta 600F; Thermo Fisher). The cell-laden samples were dehydrated by ethanol washing steps on a shaker (2 × 10 min PBS, 15 min 50% ethanol/MiliQ, 10 min 70% ethanol/MiliQ, 10 min 80% ethanol/MiliQ, 10 min 90% ethanol/MiliQ, 10 min 95% ethanol/MiliQ, 3 × 10 min 100% ethanol). The samples were dried with the critical point dryer (EM CPD300, Leica) and were gold sputtered. Samples were visualized with SEM in low vacuum, using an electron beam of 10 kV and low-vacuum secondary electron (LFD) and electron backscattered diffraction (EBSD) detectors, visualized with a yellow and blue filter respectively. Images were taken at different representative locations at multiple magnifications (100×, 1000×).

2.5. (Immuno)histochemistry

All samples were fixed in 4% paraformaldehyde solution for 20 min at room temperature (RT) and subsequently washed with PBS. All samples were stored at 4 °C until further staining.

2.5.1. 2D cell cultures

Cell cultures on coverslips were blocked using a 2% PBS/bovine serum albumin (BSA) solution for 30 min. The cells were stained with anti-CD31, anti-VE-Cadherin, anti-α-SMA, anti-PDGFrβ, anti-γH2AX, and anti-Ki67 overnight at 4 °C (Table S4, Supporting Information). Thereafter, the staining solution was removed and the coverslips were washed with PBS. Secondary antibody incubation was performed for 1 h at RT (Table S4, Supporting Information). The coverslips were washed with PBS and counterstained with DAPI for 5 min. Coverslips were mounted on microscope glass with Mowiol 4–88. Samples were stored at 4 °C prior to imaging.

2.5.2. 2D Hemodynamically Loaded Slides

Cells were blocked using 2% BSA/PBS for 30 min at RT. Cells were stained for anti-CD31 and anti-VE-cadherin (Table S4, Supporting Information) overnight 4 °C. Thereafter, the cells were washed with PBS and secondary antibody incubation (Table S4, Supporting Information) was performed for 1 h at RT. DAPI was used as counterstaining and channels were filled with Mowiol 4–88. Samples were stored at 4 °C.

2.5.3. 3D Organoid Cultures

Cells were blocked and permeabilized using 3% FBS, 1% BSA, 0.5% Triton x-100 and 0.5% Tween in PBS for 2 h at RT. 3D cell cultures were stained with anti-CD31 and anti-PDGFrβ antibodies (Table S4, Supporting Information) for 2 h at RT. The cells were washed with PBS-/Tween and secondary antibody incubation was performed for 2 h at RT. DAPI was used as counterstaining and 3D cell cultures were mounted with Mowiol4-88. Samples were stored at 4 °C prior to imaging.

2.5.4. Paraffin Sectioning of 3D Grafts

Grafts were embedded into 25% agarose gel to protect the graft material during tissue processing steps. Grafts were processed (Leica EM tissue processor, overnight without formalin) and subsequently embedded in paraffin. Sections (7×10^{-6} m thickness) were deparaffinized and citrate buffer was used for antigen retrieval for 20 min. Sections were subsequently blocked in 2% BSA/PBS and stained with anti-CD31, anti-PDGFrβ, anti-collagen IV and anti-α-SMA (Table S4, Supporting Information) overnight at 4 °C. Constructs were washed with PBS and secondary antibody staining (Table S4, Supporting Information) was performed for 1 h at RT. DAPI was used as counterstaining and constructs were mounted with Mowiol 4–88. In addition, paraffin sections were stained for hematoxylin and eosin (H&E). Samples were stored at 4 °C prior to imaging.

2.5.5. Whole Mount Staining of 3D Grafts

Grafts were blocked using a 2% PBS/BSA solution for 30 min. The grafts were stained with anti-CD31, anti-VE-Cadherin anti-collagen IV and anti-α-SMA (Table S4, Supporting Information) overnight at 4 °C. The staining solution was removed, and the coverslips were washed with PBS. Secondary antibody incubation (Table S4, Supporting Information) was performed for 1 h at RT. The constructs were washed with PBS and counterstained with DAPI. Constructs were mounted on microscope glass with Mowiol 4–88. Samples were stored at 4 °C prior to imaging.

2.5.6. Imaging and Analysis

Imaging was performed using the Leica Confocal SP8× (10×, 20× magnifications), the Leica Thunder microscope (10×, 20× and 40× magnifications for 3D organoid cultures, paraffin sections, Ibidi slides and 3D grafts) and the Olympus BX51 microscope (4× and 10× magnifications for 2D cell cultures). Images were analyzed using ImageJ software (V1.47). 3D images were composed in LASX (version 3.5.7.23225).

2.5.7. Statistical Analysis

The statistical analyses were performed using Graphpad Prism (version 8.3). Values are shown as individual data points with mean±SEM. Prior to statistical testing, outliers were removed from the results when detected using a Grubbs' test (alpha = 0.05). The paired, two-sided t-test and the ordinary one-way ANOVA test with Tukey post hoc test were used when appropriate. Experiments were performed at least in triplicate. The detailed sample size for each result is listed in the legend of the figures. A p-value of $p \leq 0.05$ was accepted as statistically significant.

3. Results

3.1. Generation and Characterization of Human iPSC-Derived Blood Vessel Organoids

Vascular organoids were generated according to the hiPSCs differentiation protocol described by Wimmer et al.[28] Gene expression profiling (Figure S1c, Supporting Information) showed steady increase in the expression of EC markers CD31 and VE-cadherin, as well as an increase in expression of MC markers PDGFrβ and ACTA2 over time during the differentiation process. In addition, EC progenitor marker CD34 increased during vascular lineage promotion and decreased during maturation of the vascular networks. In line with these differentiation steps, iPSC specific marker expression decreased over time (NANOG and OCT4) while expression of mesoderm markers (SLUG, SNAIL and TWIST) showed a positive parabolic curve with a peak expression at day 11 (Figure S2b, Supporting Information). The presence of ECs and MCs was further supported by whole-mount staining of the vascular organoids at day 21; ECs and MCs were visualized by CD31 and PDGFrβ staining, respectively, forming a dense vascular network (Figure S1d,e, Supporting Information). Cross-section images of the vascular networks confirm lumenization of the vascular networks and close proximity between ECs and MCs within the vessel structures, despite the absence of flow (Figure S1f,g, Supporting Information). These findings indicate that the iPSC to vascular organoid differentiation protocol as described by Wimmer et al. was successfully reproduced. At day 21, vascular organoids contained the highest relative numbers of vascular cells with a mature phenotype that could be used for isolation to generate pure EC and MC pools for further use.

3.2. Vascular Organoid-Derived, Cell Type-Specific Populations Can be Isolated, Cryopreserved, and Vultured in 2D Culture without Significant Loss in Cell Phenotype, Viability, or Proliferative Capacity

To investigate if both ECs and MCs populations can be isolated and cultured separately in 2D culture, fully differentiated organoids from day 18 till day 21 in 3D culture were chemically dissociated into a single-cell solution prior to cell sorting. Magnetic activated cell sorting (MACS) was used to isolate EC and MC populations from other cell types. To ensure purity of the EC and MC populations, the sorting process was repeated after expansion for two passages in 2D single culture. Cell populations were further expanded prior to cryopreservation and freezing, resulting in a biobank of pure organoid derived EC (ODEC) or organoid derived MC (ODMC) populations for further use (Figure 1a). To evaluate if EC and MC purity and phenotypes were maintained after cell sorting, cryopreservation, and prolonged 2D culture, batches of OCECs and ODMCs were thawed, followed by use in analysis and dynamic experiments up to passage 7.

Morphologically, ODECs formed a squamous-shaped, cobblestone-like single layer of cells when cultured on a gelatin coated 2D surface, similar to static 2D culture of primary human ECs (Figure 1b,c). ODMCs became elongated and were randomly distributed throughout the plate with the ability to form multilayers, similar to primary human VSMCs (Figure 1d,e). Immunofluorescent staining for EC marker VE-cadherin (Figure 1f,g) and MC marker αSMA (Figure 1h,i) confirmed the EC and MC phenotypes of ODECs and ODMCs and showed the ability of ODECs to form adherent junctions comparably to control primary cell cultures. Flow cytometry analysis using EC marker CD31 and MC marker CD140b showed limited to no cross-contamination and high purity of the ODEC and ODMC populations (Figure 1j,k).

Both ODECs and ODMCs show persistent high viability (**Figure 2**a,b) and high proliferative capacity (based on DNA content assessment and Ki67 nucleus staining, Figure 2c) over different passages (5–7) in prolonged 2D single culture. Both ODECs and ODMCs showed no DNA damage, based on γH2AX nucleus staining quantification that was comparable to HUVECs and VSMCs at passage 4 (Figure 2d). Doxorubicin treated pericytes were used as a negative control. In addition, qPCR analysis (Figure 2e) showed increased expression of EC markers (VE-cadherin and CD31) in ODECs similar to HUVECs compared to ODMCs and pericytes. Visa versa, expression of both mural cell marker PDGFrβ and VSMC marker ACTA2 were increased in ODMCs similar to primary cell cultures of human pericytes and VSMCs, compared to HUVECs and ODECs.

3.3. Endothelium Formed by ODECs Is Shear Stress Responsive and Can Actively Maintain Endothelial Barrier Function in 2D Assay Evaluation

To evaluate the shear stress responsiveness of ODECs, the Ibidi pump/slide system was used to expose ODEC monolayers to shear stress (1.5 Pa) for 48 h. A static condition was included as control. Bright field microscopy evaluation (**Figure 3**a,b) showed that ODECs subjected to shear stress become elongated and actively aligned in the direction of the flow, whereas static ODECs retained their cobblestone morphology. This was further confirmed by immunofluorescent staining (Figure 3c,d) of EC marker CD31 (green) and cytoskeleton fibers (f-actin; red) demonstrating cell alignment and orientation parallel to the direction of the flow. Similarly, qPCR results show upregulation of shear stress responsive genes KLF2, COX2 and eNOS in ODEC 2D cultures exposed to shear stress compared to static controls (Figure 3e, dotted line). Significant downregulation of pro-inflammatory genes VCAM and IL-8 were observed in ODECs exposed to shear stress compared to static controls, whereas MCP1 expression was not significantly affected (Figure S3a, Supporting Information). Exposure to shear stress did not significantly affect expression of EC specific markers VE-cadherin and CD31 (Figure S3b, Supporting Information).

Next, the ability of ODECs to form an endothelial barrier was studied using a trans-endothelial electrical resistance (TEER) assay. Endothelial barrier integrity of ODECs increased over 4 d and stabilized after reaching confluency (Figure 3f). HUVECs were used as a positive control and showed similar results to ODECs. To evaluate the potential of ODECs to regulate and maintain resistance and barrier function, we

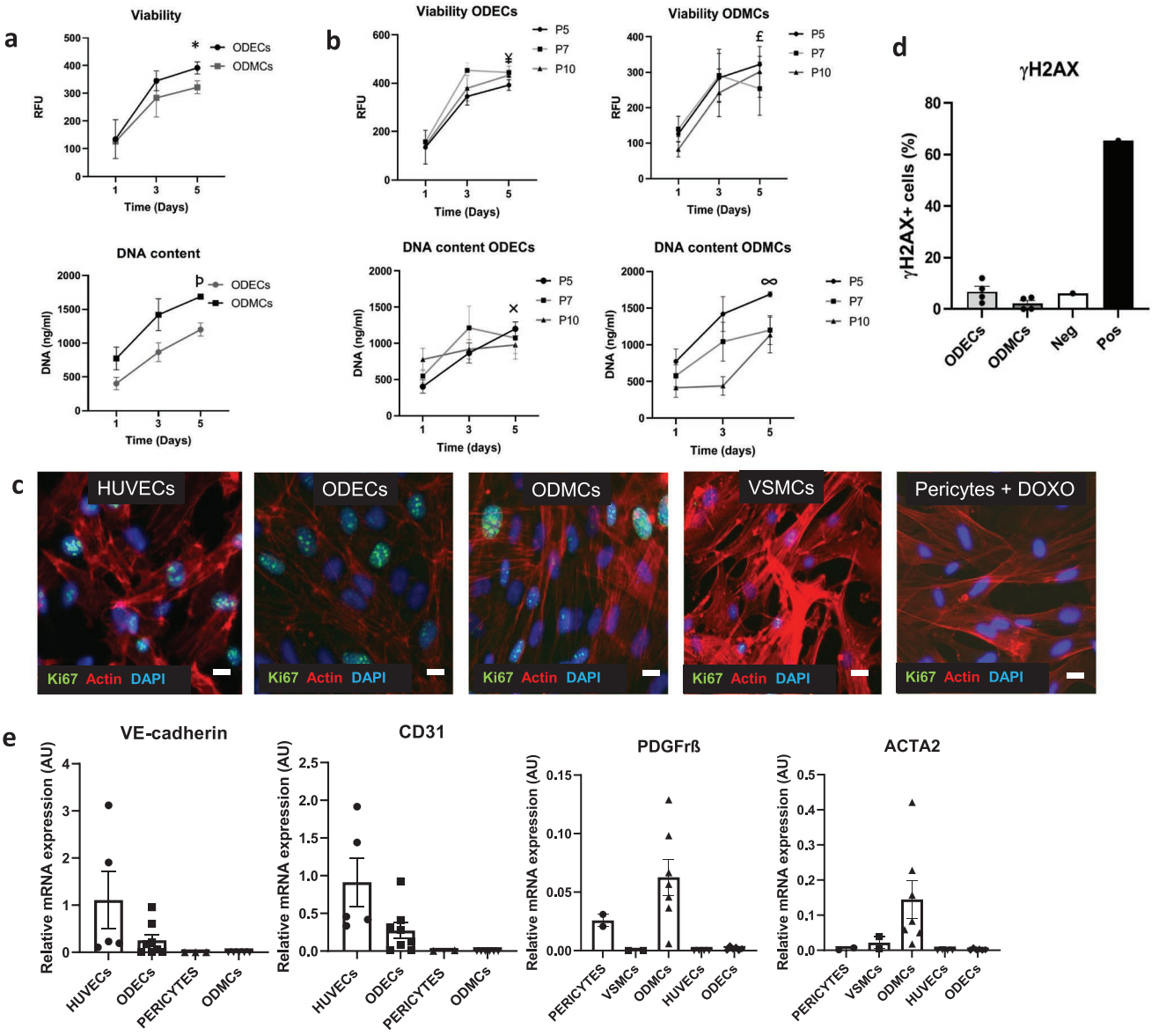

Figure 2. Organoid derived vascular cell populations preserve specific vascular cell type markers, viability and proliferative capacity. a) Results of PrestoBlue viability assay and PicoGreen proliferation assay for passage 5. Results are presented as mean ± SEM, $n = 6$, one-way ANOVA with Tukey post hoc test. $^{*}p < 0.01$ for ODECs compared to day 1 and $p < 0.05$ for ODMCs compared to day 1. $^{\flat}p < 0.01$ for both ODECs and ODMCs compared to day 1. b) Results of PrestoBlue viability assay and PicoGreen proliferation assay for multiple passages of ODECs and ODMCs. Results are presented as mean ± SEM, $n = 6$, one-way ANOVA with Tukey post hoc test $^{¥}p < 0.001$ for P5 and P7 compared to day 1. $p < 0.0001$ for P10 compared to day 1. $^{£}p < 0.05$ for P5 and P10 compared to day 1. $\times p < 0.01$ for P5 compared to D1. $^{\infty}p < 0.01$ for P5 compared to day 1 and $p < 0.05$ for P10 compared to day 1. c) Immunofluorescent stainings for proliferation marker Ki67 (green), counterstained with phalloidin (red), and DAPI (blue). HUVECs and VSMCs were used as positive control and pericytes + 0.1×10^{-6} M doxorubicin (DOXO) were used as a negative control. Scale bar represents 20 µm. d) Quantification of γH2AX positive cells. Pericytes cultured in absence (neg) or presence (pos) 0.1×10^{-6} M doxorubicin for 72 h are used as positive control for DNA damage (γH2AX). Results are presented as mean ± SEM, $n = 4$ (ODECs and ODMCs) and $n = 1$ (control cells). e) QPCR results of ODECs, ODMCs with commercially available ECs and MCs as comparison (referred to as control; HUVECs, VSMCs and pericytes). Results are presented as mean ± SEM, $n = 5$ for control primary cell cultures and $n = 8$ for organoid-derived cells. VE-cadherin, vascular endothelial cadherin; αSMA, alpha smooth muscle actin; RFU, relative fluorescent units; VE-cad, Vascular endothelial cadherin; CD, cluster of differentiation; PDGFrβ, platelet derived growth factor receptor β; ACTA2, actin alpha 2; ODECs, organoid derived endothelial cells; ODMCs, organoid derived mural cells; HUVEC, human umbilical vein endothelial cells; VSMCs, vascular smooth muscle cells.

challenged ODEC and HUVEC monolayers with thrombin. Thrombin treatment (Figure 3g, gray area) for 30 min resulted in a significant decrease of barrier resistance in both ODECs and HUVECs. Removal of thrombin triggered barrier function restoration, resulting in complete recovery of both ODEC and HUVEC endothelial electrical resistance after 150 min (Figure 3g). These data indicate that similar to primary human ECs, ODECs can form an endothelium monolayer that is shear

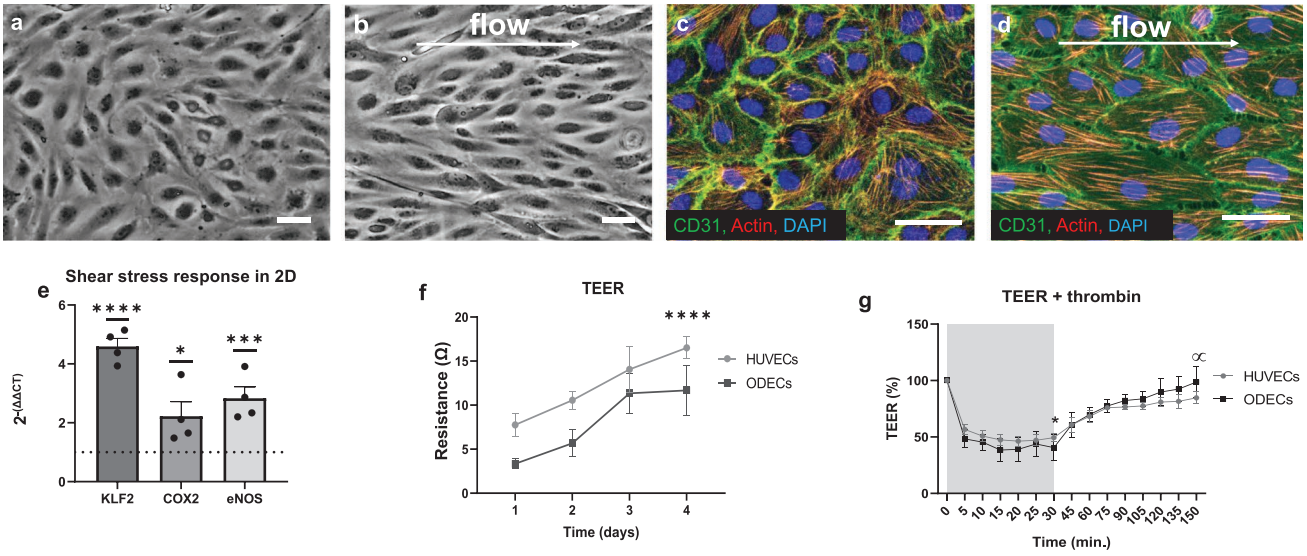

Figure 3. Functional analysis of ODECs. Bright field image of ODECs on Ibidi slide after 48 h of a) static and b) dynamic culture (1.5 Pa). Scale bar represents 50 µm. Immunofluorescent staining of ODECs for F-actin (red) and EC marker CD31 (green) after 48 h of c) static and d) dynamic culture. DAPI (blue) was used as counterstaining. e) qPCR analysis of shear stress responsive genes KLF2, COX2, and eNOS after 48 h static and dynamic culture. Dashed line represents baseline expression levels of the static culture. Data are presented as mean ± SEM, $n = 4$. One-way ANOVA with Tukey post hoc test; $^{*}p < 0.05$, *** $p < 0.001$, **** $p < 0.0001$. f) Trans-endothelial electrical resistance (TEER) of ODECs and HUVECs over time. Data are presented as mean ± SEM, $n = 4$ (HUVECs), $n = 3$ (ODECs). Paired t-test; **** $p < <0.0001$ for both HUVECs and ODECs compared to day 1. g) TEER of ODECs and HUVECs over time during 30 min thrombin treatment (gray area) and subsequent recovery. Data are presented as mean ± SEM, $n = 4$ (HUVECs), $n = 3$ (ODECs), Paired t-test; * $p < 0.001$ for HUVECs compared to 0 min and $p < 0.01$ for ODECs compared to 0 min. $^{\propto}$ $p < 0.05$ for both HUVECs and ODECs compared to 30 min. KLF2, Krüppel-like factor 2; COX2, Prostaglandin-endoperoxide synthase 2; eNOS, endothelial nitric oxide synthase.

stress responsive and establish an endothelial barrier that is actively preserved.

3.4. Organoid-Derived Vascular Cells Can be Used to Populate Small Human Artery Sized 3D-Vascular Scaffolds to Generate Biomimetic Bi-layered Human Blood Vessels

To evaluate if organoid derived vascular cells can be used to create a 3D-scaffold based biomimetic human blood vessel with dimensions relevant for human sized small arteries (2–4 mm range), ODECs and ODMCs were seeded in a layered fashion onto PCL-BU scaffolds by using fibrin as a cell carrier and cultured for 48 h in static conditions. For the control group, a combination of HUVECs and VSMCs was seeded onto similar PCL-BU scaffolds using the same protocol. Scaffolds were processed according to a predefined scheme (Figure S3c, Supporting Information).

Whole-mount staining revealed monolayer formation, with VE-cadherin expression and cell-cell junction formation on the luminal side of both 3D-vascular scaffolds seeded with control cells and organoid-derived cells (**Figure 4**a,b). Paraffin sectioning and subsequent H&E staining showed cell distribution throughout the scaffolds (Figure 4c,d, Figure S3d, Supporting Information), and the formation of MC and EC layers by immunofluorescent staining of PDGFrβ and CD31, respectively, in both control and organoid-derived blood vessels (Figure 4e,f). 3D reconstruction of the lumen area of whole-mount stained samples revealed a bi-layered configuration consisting of a monolayer of VE-cadherin positive ECs and a thicker multicellular, subendothelial layer composed of actin positive MCs, in both vascular organoid derived and control blood vessels (Figure 4g,h).

3.5. Organoid-Derived Human Blood Vessels Exposed to Flow in a Perfused Bioreactor System Preserve Intact Endothelium and Bi-Layer Configuration

Organoid- or control vascular cells seeded 3D-vascular scaffolds were mounted in a previously established bioreactor system that allows for vessel perfusion (Figure S3e, Supporting Information).[29] Luminal flow generating a gradual increase in laminar shear stress of 0.08 Pa was applied and maintained for 48 h (Table S3, Supporting Information). Immunofluorescent whole mount staining of both organoid and control vascular cells derived human blood vessels showed preserved adherent junctions (VE-cadherin) and bi-layer configuration (VE-cadherin positive endothelial monolayer, and a multicellular subendothelial layer visualized by actin staining) after 48 h of flow exposure (**Figure 5**a,b and g,h). H&E staining of cross-sections of organoid-derived and control blood vessels showed the cell distribution throughout the scaffold (Figure 5c,d and Figure S3d, Supporting Information) after 48 h of flow. the MC and EC layers were preserved after flow exposure, as shown by immunofluorescent staining of ECs (CD31) and MCs (PDGFrβ) in both control and organoid-derived human blood vessels

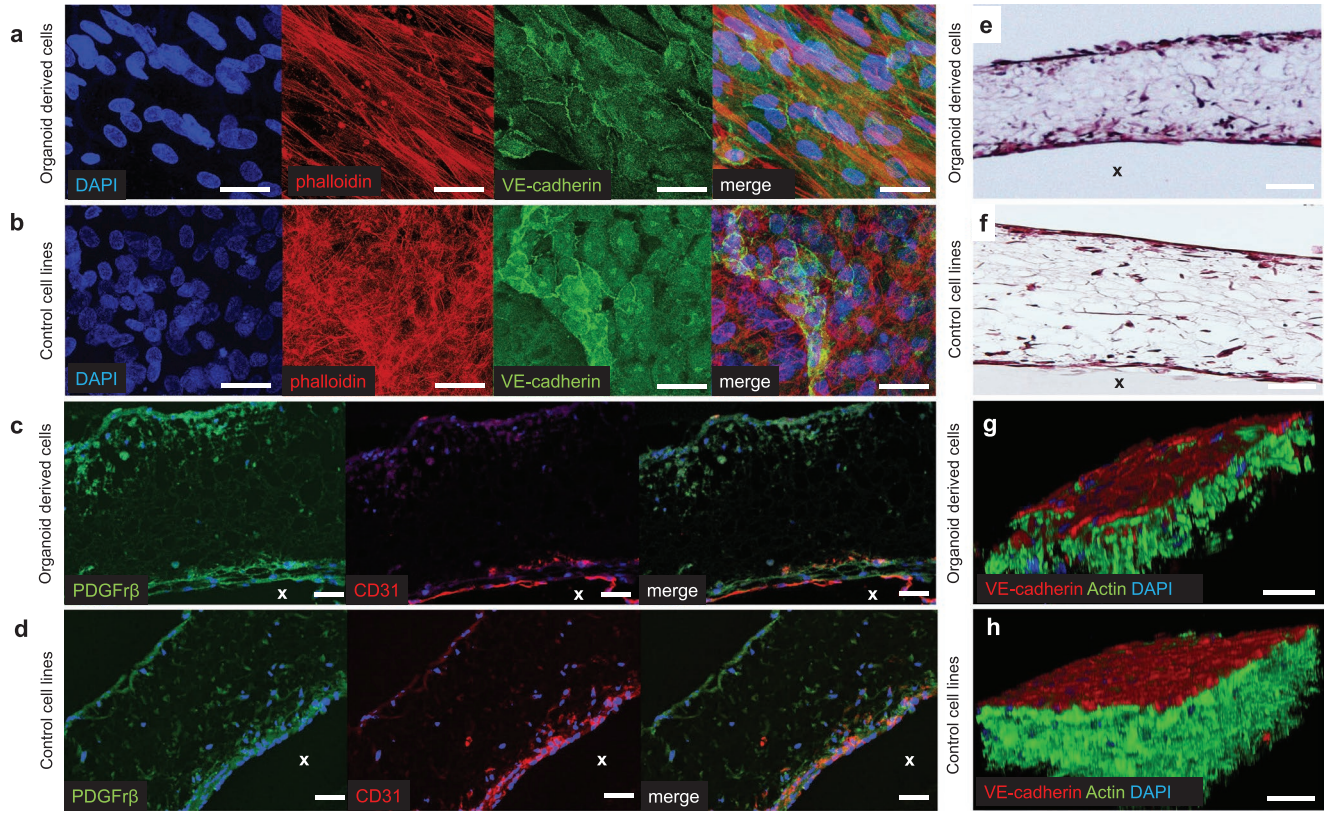

Figure 4. Evaluation of vascular grafts in static culture. *En-face* Immunofluorescent whole-mount staining of a vascular graft seeded with a) organoid-derived cells and b) control primary cell cultures with actin phalloidin (red) and EC marker VE-cadherin (green) signal after 48 h of static culture. DAPI (blue) was used to identify cell nuclei. Scale bar represents 50 µm. H&E staining of vascular graft seeded with c) ODECs and ODMCs and d) control primary cell cultures after 48 h of static culture. Scale bar represents 50 µm. Cross-sectional immunofluorescent staining of vascular grafts, seeded with e) ODECs and ODMCs and f) control primary cell cultures after 48 h of static culture. Stained with anti-PDGFrβ (green), anti-CD31 (red), and DAPI (blue). X indicates the lumen area and scale bar represents 50 µm. 3D images of whole mount staining of vascular graft seeded with g) ODECs and ODMCs and h) control primary cell cultures after 48 h of static culture immunostained for VE-cadherin (red), actin (green), and DAPI (blue). Scale bar represents 50 µm. PDGFrβ, platelet derived growth factor receptor β; VE-cad, vascular endothelial cadherin; CD, cluster of differentiation.

(Figure 5e,f). PCL-BU grafts were analyzed before seeding using SEM (**Figure 6**a,b).

SEM analysis of vascular organoid blood vessels showed a continuous lining of the luminal side of the scaffold in static culture (Figure 6c), which was preserved after 48 h of dynamic culture (Figure S3f, Supporting Information). Increased collagen IV deposition in dynamic conditions was shown by immunofluorescent staining in both organoid-derived and control human blood vessels (Figure 6d–g). mRNA analysis of shear stress responsive genes including KLF2, COX2 and eNOS showed no significant increase in expression in both organoid derived and control blood vessels in response to flow (Figure 6h). However, flow increased the expression of calponin in organoid-derived human blood vessels, whereas calponin levels in control human vessels remained unchanged (Figure 6h). Expression levels of cell specific markers were preserved in both organoid derived and control human vessels after 48 h of flow (Figure S3g, Supporting Information). Similarly, dynamic culture did not affect the mRNA level of multiple ECM components in both organoid derived and vascular control human vessels (Figure 6i).

4. Discussion

The new method developed in this study uses hiPSC-organoid derived vascular cells to create for 3D-scaffold based tissue engineering to create a perfusable human blood vessel model that recapitulates the bi-layer architecture of native vessels. The hiPSC vascular organoid-derived pipeline eliminates the need for establishing and maintaining two separate hiPSC-differentiation cultures. The resulting system offers a complex bioreactor model to meet the growing demand for in vitro testing of different scaffold prototypes for the emerging field of in situ tissue engineering.[6,7] This model may be used in combination with patient-derived hiPSCs to enable to study the role of hemodynamics in driving genetic vascular disease and its impact on vascular regeneration.

4.1. Perfused 3D-Scaffold Based Human Blood Vessel Model

Although multiple human 2D and 3D-scaffold based vascular platforms have been described in literature, most of these use

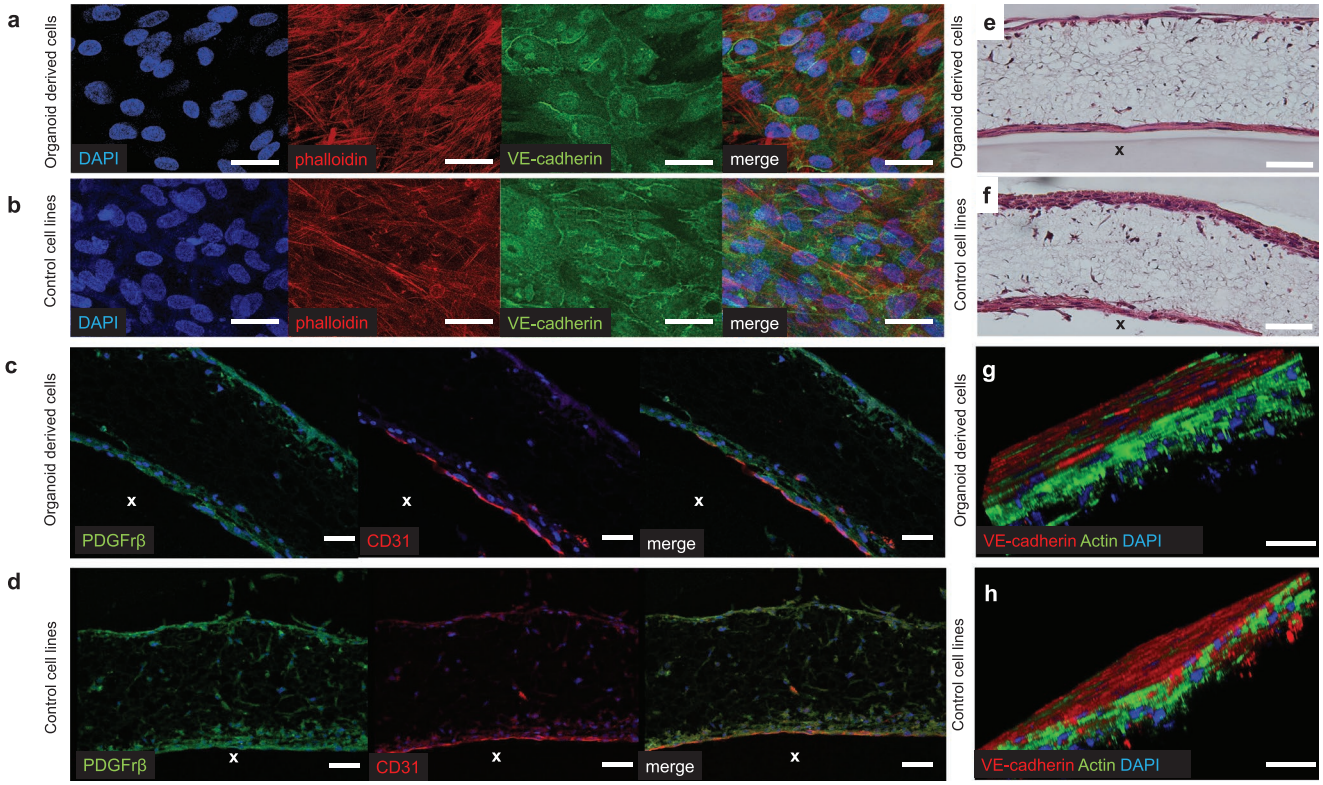

Figure 5. Evaluation of vascular grafts exposed to 48 h of flow. *En-face* Immunofluorescent whole-mount stainings of a vascular graft seeded with a) organoid-derived cells and b) control primary cell cultures with phalloidin (red) and EC marker VE-cadherin (green) after 48 h of dynamic culture (gradually increased up to 0.08 Pa, Table S3, Supporting Information). DAPI (blue) was used to identify cell nuclei. Scale bar represents 50 µm. H&E staining of vascular graft seeded with c) ODECs and ODMCs and d) control primary cell cultures after 48 h of dynamic culture (0.08 Pa). Scale bar represents 50 µm. Cross-sectional immunofluorescent staining of vascular graft, seeded with e) ODECs and ODMCs and f) control primary cell cultures after 48 h of dynamic culture (0.08 Pa). Stained with anti-PDGFrβ (green), anti-CD31 (red), and DAPI (blue). X indicates the lumen area and the scale bar represents 50 µm. 3D images of whole mount staining of vascular graft seeded with g) ODECs and ODMCs and h) control primary cell cultures after 48 h of dynamic culture immunostained for VE-cadherin (red), actin (green), and DAPI (blue). Scale bar represents 50 µm. PDGFrβ, platelet derived growth factor receptor β; VE-cad, vascular endothelial cadherin; CD, cluster of differentiation.

primary vascular cells (e.g., aorta derived VSMCs and HUVECs) as a cell source[32–34] or focus on assessment of a single cell type in response to an isolated hemodynamic aspect without fully recapitulating the vessel architecture.[26,35,36] Over the past years, more complex systems have been described, improving the biological relevance of these systems by mimicking the native bi-layer architecture to allow the natural paracrine, ion channel-based and receptor-ligand interactions between ECs and VSMCs,[37] which have been shown to play critical roles in vasomotion, homeostasis, tissue adaptation in disease condition and vessel regenerative and hemodynamic response.[40,41] Still, only a limited number of these used iPSC-derived vascular cells to create a bilayered TEVG.[38,39,42] Nakayama et al. successfully produced bilayered aligned nanofibrillar collagen graft, using iPSC-derived vascular cells as a cell source and demonstrated in their experiments that EC-seeded aligned scaffolds significantly reduced inflammatory response, based on monocytes adhesion and thus provided an atheroprotective function, even without application of flow on these constructs .[38] In 2019, the group of Generali et al. also demonstrated a PGA- based bilayered vascular graft based on both iPSC-derived endothelial cells and vascular smooth muscle cells under flow. These constructs were kept in culture up to nine weeks resulting in a construct with a thick layer of extracellular matrix, containing a αSMA-positive layer in the interstitium and a thin luminal layer of vWF-positive endothelial cells, approximating the architecture of native vessels.[39] The 3D-scaffold based model presented in this study also offers a human blood vessel analogue that mimics the native vessel's bi-layer tissue organization, which is successfully preserved under flow and derived from a single differentiation protocol. The use of iPSC vascular organoid derived cells for graft creation as presented in the current study, could further open up new possibilities for tissue engineering of patient-specific vascular grafts for disease modeling. It would be particularly suitable in facilitating studies that require the natural cross talk between the endothelium and medial layer to closely represent the human disease condition in vivo.

Various designs, fabrication methods and materials have been previously used to generate the vascular tubular scaffold backbone.[43–45] In our experiments, the suitability of ODECs and ODMCs for vascular TE was tested on a small-diameter electrospun PCL-BU based scaffold with collagen I and

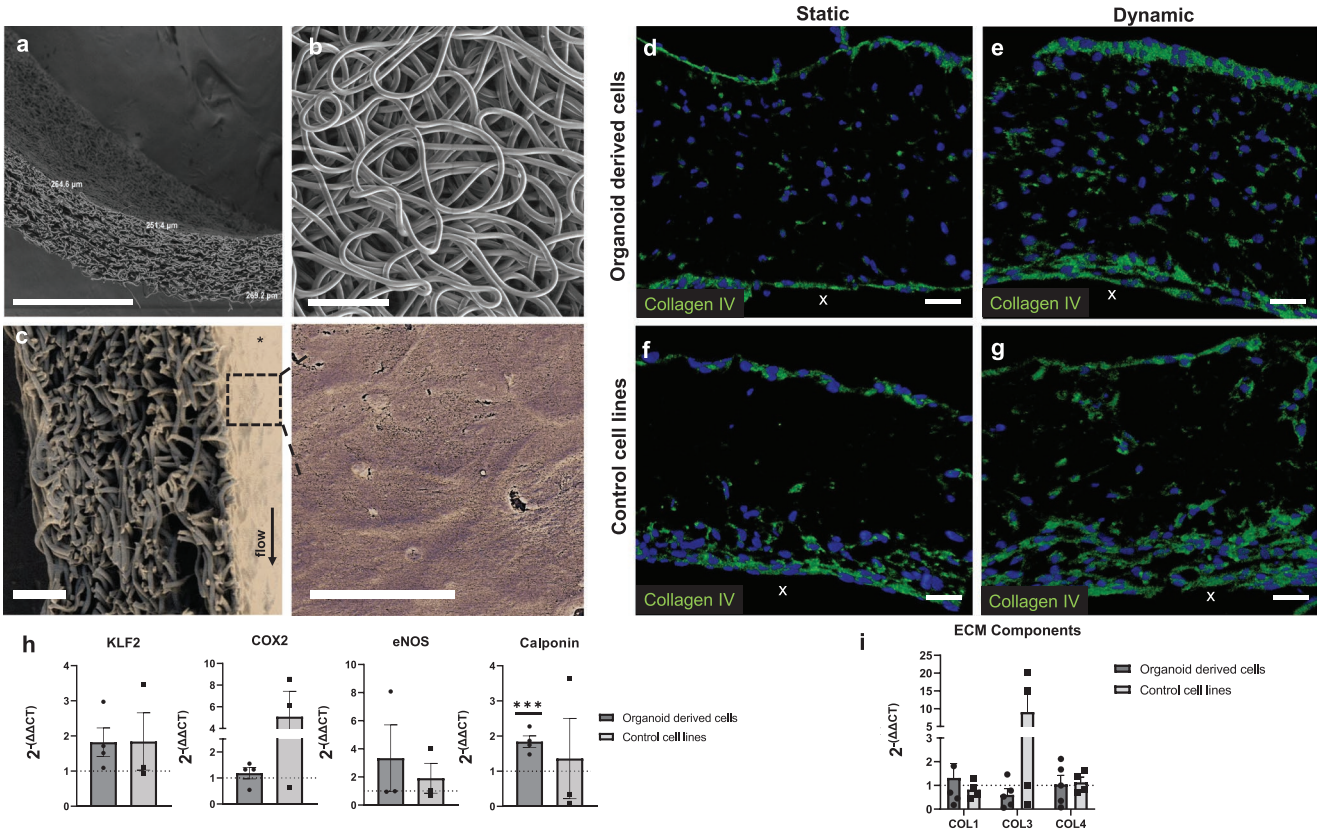

Figure 6. Flow response of vascular grafts. a) A representative SEM picture of a scaffold prior cell seeding showing an average wall thickness of 268 ± 8 µm. b) SEM picture of a scaffold prior seeding showing an isotropic fiber orientation with an average fiber diameter of 4.1 ± 0.2 µm at the luminal side of the scaffold. c) The left SEM picture of a scaffold seeded with ODECs and ODMCs demonstrates a confluent layer of cells at the luminal side of the scaffold. Detailed *en-face* SEM picture of the graft's endothelium at the right. Cross-sectional immunofluorescent staining of a vascular graft, either seeded with d,e) ODECs and ODMCs or f,g) HUVECS and VSMCs after 48 h of static and dynamic culture, stained with anti-collagen IV (green) and DAPI (blue). X Indicates lumen and scale bar represents 50 µm. qPCR analysis of h) shear stress responsive genes KLF2, COX2, eNOS, and calponin and of i) ECM component genes Collagen I, Collagen II, and Collagen IV after 48 h static and dynamic culture. Dotted lines represent gene expression at static culture levels. Data are presented as mean ± SEM, $n = 4$ (organoid-derived graft), $n = 4$ (control graft). Paired *t*-test; $^{***}p < 0.001$. KLF2, Krüppel-like factor 2; COX2, Prostaglandin-endoperoxide synthase 2; eNOS, endothelial nitric oxide synthase; Col, collagen.

fibronectin coating similar to Pennings et al.,[29] while cells were seeded in an additional fibrin carrier solution. The addition of fibrin was chosen because fibrin matrix support has been shown to improve vascular stability upon implantation and enhance EC retention under flow.[46–48] The use of fibrin as a cell carrier prevents loss of cell solution and ensures homogeneous cell distribution.[49,50] The selection of the PCL-BU material and fiber diameter as well as the random fiber orientation and scaffold thickness are based on findings of the successful application of this particular design in vascular tissue engineering by our group previously.[51–53] Furthermore, PCL-BU is an easy to functionalize polymer, which has been proven to be biocompatible and biodegradable in the local environment of the vascular system.[54]

We observed that ODECs, similar to HUVECs in the control grafts, maintained CD31 EC marker expression, VE-cadherin expression in cell-cell junctions, and form a consistent monolayer when seeded into the 3D scaffolds. ODMCs, similar to VSMCs in control grafts, form tissue layers at the basal side of the endothelium, and are located dispersed throughout the scaffold wall. The resulting bi-layered (confluent endothelium and basal medial layer) configuration is in line with what was previously observed in static studies using the same bioreactor setup and PCL grafts seeded with endothelial colony forming cells (ECFCs) and VSMCs derived from mesenchymal stem cells (MSCs).[29] The bi-layered configuration with an intact endothelial monolayer on the luminal side of the scaffold on top of ODMCs or VSMCs was sustained when exposed to flow conditions (0.08 Pa). VE-cadherin signal remained localized in cell-cell junctions, and confluent luminal side coverage was confirmed by SEM analysis, indicating that the endothelium and the media was not disrupted after 48 h of flow exposure in both the organoid derived and control grafts. However, no flow-induced alignment was observed for both ODECs and HUVECs in the 3D culture, despite the observed shear stress sensitivity in 2D. The current shear stress levels of 0.08 Pa as applied in the bioreactor may not have been sufficient to provoke EC re-orientation. Furthermore, the high ODECs or HUVECs seeding density that was used may also have impeded the flow induced alignment, as was observed previously.[55]

ECs are known to regulate phenotype switching of VSMCs.[56,57] In our experiments a significant upregulation

of the contractile marker calponin was observed, implying a transition toward a contractile phenotype of the ODMCs in response to shear stress exposure. In contrast, no upregulation in calponin expression was observed after hemodynamic loading of control graft. This lack of response may be due to differences in basal expression levels. Basal (nonflowed) Calponin mRNA levels were significantly lower in HUVECs/VSMCs grafts versus organoid-derived grafts (mean ± SEM = 0.00023 ± 0.00031 versus 0.0019 ± 0.0011, for cell-line versus organoid derived respectively, P = 0.02), implying that Calponin was hardly transcribed in the aorta derived VSMCs compared with ODMCs. The plasticity of graft seeded cells to in vivo adapt to local hemodynamic forces is critical for long term graft function and survival. In future studies, we will further assess the capacity of scaffold seeded ODECs to regulate phenotype transition of ODMCs in response to shear stress exposure.

4.2. Vascular Organoid-Derived ODECs and ODMCs as a Cell Source for Model Building

Differentiation protocols for iPSC-derived ECs and iPSC-derived MCs have been previously reported.[9,10,14–21] Although hiPSC-derived vascular cells are used for in vitro studies, only a select number of studies report their application in hierarchical vascular tissue engineering. Gui et al., developed hiPSC-TE vascular constructs under static culture conditions by seeding hiPSC-VSMCs on polyglycolic acid (PGA) scaffolds followed by eight weeks of culture under static conditions. Scaffold-seeded hiPSC-VSMCs retained expression of VSMC contractile markers and collagen was deposited on scaffold fibers.[27] Similarly, Sundaram et al. differentiated hiPSCs into mesenchymal progenitors and seeded these on PGA polymer scaffolds to develop tissue engineered vessels in a bioreactor that could provide pulsatile cyclic stretch. The use of PDGF-BB in the culture medium secured VSMC lineage specification of hiPSC-derived mesenchymal progenitors. This together with eight weeks of cyclic stretch exposure, promoted expression of typical VSMC markers and increased collagen deposition.[25] However, no introduction of hiPSC-ECs and subsequent endothelialization of the 3D scaffold was reportedly achieved in these studies. Studies that investigate the application of hiPSC-EC in tissue engineered vessel is limited to a report by Tan et al. who demonstrated that PCL-gelatin scaffolds supported hiPSC-EC growth, phenotype retention and function in vitro.[26] Nevertheless, reports that demonstrate the combined application of both hiPSC-ECs and hiPSC-MCs for tissue engineering of vascular structures for the creation of perfused human blood vessel models, are currently lacking.

Our perfused hiPSC human blood vessel model from organoid-derived vascular cells offers a 3D-scaffold based bi-layer vessel mimic in a perfusable bioreactor system that could be particularly useful as a patient-specific in vitro disease model. For example hiPSCs derived from CVD patients with familiar genetic mutations or SNPs linked to early onset of coronary artery disease and endothelial dysfunction, may be used to model disease arteries to study their impact of on disease mechanisms or regenerative capacity. In relation to the latter, patient-cell derived vascular disease models are particularly relevant in combination with the emerging treatment strategy of in situ vascular tissue engineering, which is heavily reliant on the healing capacity of the recipient's cells.[58] In this study, we investigated if pools of hiPSCs vascular organoid derived ECs and MCs can be harvested and used as a cell source for in vitro tissue engineering of small-diameter (3 mm) vascular constructs with native-like tissue hierarchy. In the native condition, the process of vascular cell differentiation from a progenitor state involves continuous guidance via cell contact and paracrine interaction between different cell types in the direct environment of the developing vasculature. Indeed multiple studies have also demonstrated that ECs and mural cells (MCs, or pericytes and VSMCs) interactions are critical for EC differentiation and function, and vice versa.[59–62] The culture protocol used in this study for hiPSC-derived blood vessel organoids was first described in a recent paper by Wimmer et al.[28] Vascular differentiation from the mesoderm phase in this system takes place in a 3D environment in which the EC and MC lineages can establish with natural cross cell type interactions and eventually forms 3D structures that resemble a vascular network after 18–21 d of culture. Similar to previously reported hiPSC-derived EC and hiPSC-derived MCs, ODECs and ODMCs isolated from these vascular organoids recapitulate the morphology of human primary ECs (HUVECs) and MCs (aorta derived VSMCs) in 2D culture and express the corresponding characteristic markers.[23,24] For the in situ vascular tissue engineering strategy, the capacity for fast in situ formation of the endothelial monolayer barrier after scaffold implantation and subsequent active preservation is crucial for the prevention of blood clotting and uncontrolled, adverse interactions of circulating immune cells and blood components with polymer structures,[63,64] and thus is essential for protection against loss of patency. Similarly, the endothelial barrier is critical for the function of healthy vessels and is often compromised in CVD. Our experiments indicate that the ODECs can form confluent endothelial monolayers with well-established VE-cadherin adherens junctions and cobblestone morphology similar to HUVECs. Gradual increase of TEER signal indicates effective buildup of the endothelial barrier by ODECs over several days post seeding, also similar to HUVECs. More strikingly, confluent ODEC monolayers have the capacity to restore the endothelial barrier resistance actively and completely after thrombin challenge, similar to HUVEC monolayers. This innate restorative capacity of ODECs mimics the in vivo condition of healthy vessels. Future studies should explore more aspects that define the functionality of the endothelium, including blood contact reponse and NO production under flow, to aid in further development and optimization of hiPSC organoid-derived macrovascular models,

Although cell seeding on scaffolds produced vascular grafts with a media composed of multiple layers of ODMCs, the scaffold's central core remained sparse of cells. This was also observed for grafts seeded with primary VSMCs, indicating that the observed lack of cells was not due to the iPSC origin of ODMCs. In our current seeding procedure, ODMCs and VSMCs were seeded on the scaffold's luminal and adventitial surface. Penetration of cells was feasible by design, as the scaffold's pores were on average >15 μm in diameter. Indeed, ODMCs and VSMCs tissue formation was observed inside the scaffold, expanding from the luminal and adventitial sides.

The current protocol includes 7 d of static culture after seeding before hemodynamic loading. More time may be required for ODMC and VSMC expansion to reach the core region. Although the scaffold's thickness (250 μm) does not exceed the hypothetical maximal diffusion distance for cell survival (1 mm), nutrients and oxygen may become less available at the center once tissue structures are established in the border regions, thus reducing further expansion efficacy. To promote core cellularization, a protocol may be adapted in which only the luminal side is seeded with ODMCs/VSMCs, leaving an adventitial route of entry for the medium, followed by a prolonged static culture step.

The ODMCs/ODECs grafts were exposed to 0.08 Pa of shear stress. This is only slightly lower than the levels found in veins (0.1–0.6 Pa),[3] which makes the model with the current flowing protocol suitable to study for example, venous disease. The current model can be further adapted to achieve a higher range of shear stresses by increasing viscosity of the flow medium[4] or by application of higher flow rates. The latter will require a prolonged culture step after scaffold seeding, to allow more time for the deposition of the basement membrane that is essential for the strengthening of the vessel wall. Our data indicate, that challenging ODECs/ODMCs or HUVECs/VSMCs grafts with 0.08 Pa shear stress during this process can accelerate the build-up of collagen IV, a vascular basement membrane component vital for cell adhesion and stabilization (Figure 6d–g). This observation is in line with previous publications, which have shown that shear stress stimulation during graft culture enhances several important aspects of graft maturation relevant for enhancing vascular strength.[5–7] Future studies will further explore prolonged static culture in combination with and without prolonged 0.08 Pa of shear stress exposure for the improvement of ODECs/ODMCs vascular graft strength to achieve higher shear stress ranges with this model.

In vivo, ECs in 3D-scaffold based grafts are required to adapt to local hemodynamic conditions, such as local shear stress levels to preserve vascular and endothelial integrity and barrier function. Depending on the location on the vascular tree, shear stress levels vary between 0.2–1.6 Pa,[65] and deviation in shear stress leads to onset and progression of CVD. In our experiments, ODECs subjected to relatively high shear stress (1.5 Pa) for 48 h responded like HUVECs, with actin stress fiber formation and cell alignment with the flow direction, whereas the integrity of the monolayer and adherens junctions was maintained. These findings are supported by the detected upregulation of shear stress responsive genes KLF2, COX2 and eNOS, upon subjection to flow. Increased expression of the KLF2 transcription factor expression is a key mechanism of the endothelium to mediate a protective anti-inflammatory response to shear stress via downregulation of (secreted) inflammation associated factors such as the cytokines IL8, MCP1 and membrane VCAM that facilitates immune cell adhesion.[66,67] In ODECs, like in HUVECs, shear stress was previously shown to indeed reduce IL8, MCP1 and VCAM expression compared to static conditions.[68] Together, our data indicate that ODECs have the capacity to adequately adapt to shear stress conditions, similar to primary human endothelial cells.

Combined, these findings show that the use of ODECs in the perfused human blood vessel model, could therefore make the platform suitable for testing endothelialization and EC response to shear stress of different 3D-scaffold designs, and could be used for the creation of vascular disease models in which endothelial barrier function and shear stress adaptation are used as vital assay readouts.

In conclusion, the hiPSC derived vascular organoid cells can be successfully used as a source of functional, flow-adaptive vascular cells for tissue engineering of a perfused human blood vessel model. The methods may be used to establish an in vitro model for (cardio)vascular diseases for personalized drug treatment research, using hiPSCs from patients with genetic CVD. In addition, it may also be used as a platform for testing new scaffold designs for the in situ TE strategy in which the impact of genetic disease on the regeneration capacity of CVD patients can be evaluated.

Supporting Information

Supporting Information is available from the Wiley Online Library or from the author.

Acknowledgements

The authors would like to thank Rob Driessen for his help with the flow pump system and the critical point dryer. In addition, the authors would like to thank Krista den Ouden for her help with sectioning and staining of the 3D samples. This work was funded by the REGMEDXB cardiovascular moonshot consortium, the NWO vidi grant (no. 91714302 to CC), the TKI Health Holland BIORAB project (no. LSHM19032), and the InSiTeVx project (436001003), which is financially supported by ZonMw within the LSH 2Treat Program and the Dutch Kidney Foundation. The authors gratefully acknowledge the Gravitation Program "Materials Driven Regeneration", funded by the Netherlands Organization for Scientific Research (024.003.013).

Conflict of Interest

The authors declare no conflict of interest.

Author Contributions

E.M.M. and S.E.K. are co-first authors, C.G.M.v.D. and R.G.C.M. are co-second authors, A.I.P.M.S. and C.C. are co-last authors. K.L.C., A.I.P.M.S., M.C.V., and C.V.C.B. devised the project and the main conceptual ideas. R.G.C.M. and E.M.M. performed iPSC differentiation protocols, supervised by J.W.B. W.S. performed the electrospinning and provided the scaffolds. Static cell culture experiments were performed by E.M.M., I.C., C.G.M.D., P.J.B., and S.E.K. L.P. and V.J.C.H.K. performed dynamic cell culture experiments. E.M.M., S.E.K., and C.G.M.D. analyzed the data and wrote the manuscript, with the help of K.L.C. All the authors reviewed the final manuscript. The project was equally supervised by K.L.C. and A.I.P.M.S.

Data Availability Statement

The data that support the findings of this study are available from the corresponding author upon reasonable request.

Keywords

blood vessel organoids, endothelial cells, graft perfusion, vascular graft, vasculature

Received: May 17, 2022
Revised: September 2, 2022
Published online: October 27, 2022

[1] D. Mozaffarian, E. J. Benjamin, A. S. Go, D. K. Arnett, M. J. Blaha, M. Cushman, S. de Ferranti, J. P. Despres, H. J. Fullerton, V. J. Howard, M. D. Huffman, S. E. Judd, B. M. Kissela, D. T. Lackland, J. H. Lichtman, L. D. Lisabeth, S. Liu, R. H. Mackey, D. B. Matchar, D. K. McGuire, E. R. Mohler3rd, C. S. Moy, P. Muntner, M. E. Mussolino, K. Nasir, R. W. Neumar, G. Nichol, L. Palaniappan, D. K. Pandey, M. J. Reeves, et al., *Circulation* **2015**, *131*, e29.
[2] N. Townsend, D. Kazakiewicz, F. Lucy Wright, A. Timmis, R. Huculeci, A. Torbica, C. P. Gale, S. Achenbach, F. Weidinger, P. Vardas, *Nat Rev Cardiol.* **2022**, *19*, 133.
[3] I. W. Mak, N. Evaniew, M Ghert, *Am. J. Transl. Res.* **2014**, *6*, 114.
[4] P. Pound, R Ram, *BMJ Open Sci.* **2020**, *4*, e100041.
[5] S. Lal, A. Li, *J. Cardiovasc. Transl. Res.* **2016**, *9*, 165.
[6] D. Duran-Rey, V. Crisostomo, J. A. Sanchez-Margallo, F. M Sanchez-Margallo, *Front. Bioeng. Biotechnol.* **2021**, *9*, 771400.
[7] H. Talacua, A. I. Smits, D. E. Muylaert, J. W. van Rijswijk, A. Vink, M. C. Verhaar, A. Driessen-Mol, L. A. van Herwerden, C. V. Bouten, J. Kluin, B. F. P. In, *Tissue Eng., Part A* **2015**, *21*, 2583.
[8] S. Abdulghani, G. R Mitchell, *Biomolecules* **2019**, *9*.
[9] V. V. Orlova, F. E. van den Hil, S. Petrus-Reurer, Y. Drabsch, P. Ten Dijke, C. L Mummery, *Nat. Protoc.* **2014**, *9*, 1514.
[10] M. Shen, T. Quertermous, M. P. Fischbein, J. C Wu, *Circ. Res.* **2021**, *128*, 670.
[11] N. L'Heureux, S. Paquet, R. Labbe, L. Germain, F. A Auger, *FASEB J.* **1998**, *12*, 47.
[12] R. D. Chavez, S. L. Walls, K. O Cardinal, *PLoS One* **2019**, *14*, e0217709.-
[13] M. C. Gibbons, M. A. Foley, K. O Cardinal, *Tissue Eng., Part B* **2013**, *19*, 14.
[14] A. J. Rufaihah, N. F. Huang, J. Kim, J. Herold, K. S. Volz, T. S. Park, J. C. Lee, E. T. Zambidis, R. Reijo-Pera, J. P Cooke, *Am. J. Transl. Res.* **2013**, *5*, 21.
[15] K. D. Choi, J. Yu, K. Smuga-Otto, G. Salvagiotto, W. Rehrauer, M. Vodyanik, J. Thomson, I Slukvin, *Stem Cells* **2009**, *27*, 559.
[16] L. Wang, M. Xiang, Y. Liu, N. Sun, M. Lu, Y. Shi, X. Wang, D. Meng, S. Chen, J Qin, *Biomicrofluidics* **2016**, *10*, 014106.
[17] W. J. Adams, Y. Zhang, J. Cloutier, P. Kuchimanchi, G. Newton, S. Sehrawat, W. C. Aird, T. N. Mayadas, F. W. Luscinskas, G Garcia-Cardena, *Stem Cell Rep.* **2013**, *1*, 105.
[18] M. P. White, A. J. Rufaihah, L. Liu, Y. T. Ghebremariam, K. N. Ivey, J. P. Cooke, D Srivastava, *Stem Cells* **2013**, *31*, 92.
[19] V. V. Orlova, Y. Drabsch, C. Freund, S. Petrus-Reurer, F. E. van den Hil, S. Muenthaisong, P. T. Dijke, C. L Mummery, *Arterioscler., Thromb., Vasc. Biol.* **2014**, *34*, 177.
[20] D. Taura, M. Sone, K. Homma, N. Oyamada, K. Takahashi, N. Tamura, S. Yamanaka, K Nakao, *Arterioscler., Thromb., Vasc. Biol.* **2009**, *29*, 1100.
[21] M. Stephenson, D. H. Reich, K. R Boheler, *Vasc. Biol.* **2020**, *2*, R1.
[22] Y. K. Kurokawa, R. T. Yin, M. R. Shang, V. S. Shirure, M. L. Moya, S. C George, *Tissue Eng., Part C* **2017**, *23*, 474.
[23] S. Jang, A. Collin de l'Hortet, A Soto-Gutierrez, *Am. J. Pathol.* **2019**, *189*, 502.
[24] B. C. Dash, Z. Jiang, C. Suh, Y Qyang, *Biochem. J.* **2015**, *465*, 185.
[25] S. Sundaram, J. One, J. Siewert, S. Teodosescu, L. Zhao, S. Dimitrievska, H. Qian, A. H. Huang, L Niklason, *Stem Cells Transl. Med.* **2014**, *3*, 1535.
[26] R. P. Tan, A. H. P. Chan, K. Lennartsson, M. M. Miravet, B. S. L. Lee, J. Rnjak-Kovacina, Z. E. Clayton, J. P. Cooke, M. K. C. Ng, S. Patel, S. G Wise, *Stem Cell Res. Ther.* **2018**, *9*, 70.
[27] L. Gui, B. C. Dash, J. Luo, L. Qin, L. Zhao, K. Yamamoto, T. Hashimoto, H. Wu, A. Dardik, G. Tellides, L. E. Niklason, Y Qyang, *Biomaterials* **2016**, *102*, 120.
[28] R. A. Wimmer, A. Leopoldi, M. Aichinger, N. Wick, B. Hantusch, M. Novatchkova, J. Taubenschmid, M. Hammerle, C. Esk, J. A. Bagley, D. Lindenhofer, G. Chen, M. Boehm, C. A. Agu, F. Yang, B. Fu, J. Zuber, J. A. Knoblich, D. Kerjaschki, J. M Penninger, *Nature* **2019**, *565*, 505.
[29] I. Pennings, E. E. van Haaften, T. Jungst, J. A. Bulsink, A. Rosenberg, J. Groll, C. V. C. Bouten, N. A. Kurniawan, A. Smits, D Gawlitta, *Biofabrication* **2019**, *12*, 015009.
[30] T. Kitani, S. G. Ong, C. K. Lam, J. W. Rhee, J. Z. Zhang, A. Oikonomopoulos, N. Ma, L. Tian, J. Lee, M. L. Telli, R. M. Witteles, A. Sharma, N. Sayed, J. C Wu, *Circulation* **2019**, *139*, 2451.
[31] S. E. Koch, E. E. van Haaften, T. B. Wissing, L. A. B. Cuypers, J. A. Bulsink, C. V. C. Bouten, N. A. Kurniawan, A Smits, *J. Visualized Exp.* **2020**, https://doi.org/10.3791/61824.
[32] H. Miyachi, J. W. Reinhardt, S. Otsuru, S. Tara, H. Nakayama, T. Yi, Y. U. Lee, S. Miyamoto, T. Shoji, T. Sugiura, C. K. Breuer, T Shinoka, *Int. J. Cardiol.* **2018**, *266*, 61.
[33] T. Fukunishi, C. A. Best, C. S. Ong, T. Groehl, J. Reinhardt, T. Yi, H. Miyachi, H. Zhang, T. Shinoka, C. K. Breuer, J. Johnson, N Hibino, *Tissue Eng., Part A* **2018**, *24*, 135.
[34] T. L. Mirensky, N. Hibino, R. F. Sawh-Martinez, T. Yi, G. Villalona, T. Shinoka, C. K Breuer, *J. Pediatr. Surg.* **2010**, *45*, 1299.
[35] N. Hibino, E. McGillicuddy, G. Matsumura, Y. Ichihara, Y. Naito, C. Breuer, T Shinoka, *J. Thorac. Cardiovasc. Surg.* **2010**, *139*, 431.
[36] T. Sugiura, G. Matsumura, S. Miyamoto, H. Miyachi, C. K. Breuer, T Shinoka, *Semin. Thorac. Cardiovasc. Surg.* **2018**, *30*, 175.
[37] N. Mendez-Barbero, C. Gutierrez-Munoz, L. M Blanco-Colio, *Int. J. Mol. Sci.* **2021**, *22*, 7284.
[38] K. H. Nakayama, P. A. Joshi, E. S. Lai, P. Gujar, L. M. Joubert, B. Chen, N. F Huang, *Regener. Med.* **2015**, *10*, 745.
[39] M. Generali, E. A. Casanova, D. Kehl, D. Wanner, S. P. Hoerstrup, P. Cinelli, B Weber, *Acta Biomater.* **2019**, *97*, 333.
[40] H. C. Wu, T. W. Wang, P. L. Kang, Y. H. Tsuang, J. S. Sun, F. H Lin, *Biomaterials* **2007**, *28*, 1385.
[41] X. Dong, X. Yuan, L. Wang, J. Liu, A. C. Midgley, Z. Wang, K. Wang, J. Liu, M. Zhu, D Kong, *Biomaterials* **2018**, *181*, 1.
[42] I. Marei, T. Abu Samaan, M. A. Al-Quradaghi, A. A. Farah, S. H. Mahmud, H. Ding, C. R Triggle, *Front. Cardiovasc. Med.* **2022**, *9*, 847554.
[43] C. S. Ong, X. Zhou, C. Y. Huang, T. Fukunishi, H. Zhang, N Hibino, *Expert Rev. Med. Devices* **2017**, *14*, 383.
[44] Y. Liu, T. Nelson, J. Chakroff, B. Cromeens, J. Johnson, J. Lannutti, G. E Besner, *J. Biomed. Mater. Res., Part B* **2019**, *107*, 750.
[45] A. Rathore, M. Cleary, Y. Naito, K. Rocco, C Breuer, *Wiley Interdiscip. Rev.: Nanomed. Nanobiotechnol.* **2012**, *4*, 257.
[46] B. C. Isenberg, C. Williams, R. T Tranquillo, *Ann. Biomed. Eng.* **2006**, *34*, 971.
[47] E. D. Grassl, T. R. Oegema, R. T Tranquillo, *J. Biomed. Mater. Res.* **2002**, *60*, 607.
[48] C. Gosselin, D. A. Vorp, V. Warty, D. A. Severyn, E. K. Dick, H. S. Borovetz, H. P Greisler, *J. Surg. Res.* **1996**, *60*, 327.
[49] M. Stekelenburg, M. C. Rutten, L. H. Snoeckx, F. P Baaijens, *Tissue Eng., Part A* **2009**, *15*, 1081.

[50] A. Mol, M. I. van Lieshout, C. G. Dam-de Veen, S. Neuenschwander, S. P. Hoerstrup, F. P. Baaijens, C. V Bouten, *Biomaterials* **2005**, *26*, 3113.
[51] T. B. Wissing, V. Bonito, E. E. van Haaften, M. van Doeselaar, M. Brugmans, H. M. Janssen, C. V. C. Bouten, A Smits, *Front. Bioeng. Biotechnol.* **2019**, *7*, 87.
[52] D. J. Wu, K. van Dongen, W. Szymczyk, P. J. Besseling, R. M. Cardinaels, G. Marchioli, M. H. P. van Genderen, C. V. C. Bouten, A. Smits, P. Y. W Dankers, *Front. Mater.* **2020**, *7*, 220.
[53] T. B. Wissing, E. E. van Haaften, S. E. Koch, B. D. Ippel, N. A. Kurniawan, C. V. C. Bouten, A Smits, *Biomater. Sci.* **2019**, *8*, 132.
[54] E. E. van Haaften, R. Duijvelshoff, B. D. Ippel, S. H. M. Sontjens, M. van Houtem, H. M. Janssen, A. Smits, N. A. Kurniawan, P. Y. W. Dankers, C. V. C Bouten, *Acta Biomater.* **2019**, *92*, 48.
[55] S. Ohta, S. Inasawa, Y Yamaguchi, *J. Phys. D: Appl. Phys.* **2015**, *48*, 245401.
[56] R. J. Powell, J. L. Cronenwett, M. F. Fillinger, R. J. Wagner, L. N Sampson, *Ann. Vasc. Surg.* **1996**, *10*, 4.
[57] R. J. Powell, J. Hydowski, O. Frank, J. Bhargava, B. E Sumpio, *J. Surg. Res.* **1997**, *69*, 113.
[58] B. J. de Kort, S. E. Koch, T. B. Wissing, M. M. Krebber, C. V. C. Bouten, A Smits, *Adv. Drug Delivery Rev.* **2021**, *178*, 113960.
[59] M. M. Brandt, C. G. M. van Dijk, R. Maringanti, I. Chrifi, R. Kramann, M. C. Verhaar, D. J. Duncker, M. Mokry, C Cheng, *Sci. Rep.* **2019**, *9*, 15586.
[60] G. Chiaverina, L. di Blasio, V. Monica, M. Accardo, M. Palmiero, B. Peracino, M. Vara-Messler, A. Puliafito, L Primo, *Cells* **2019**, *8*, 1109.
[61] H. Gerhardt, C Betsholtz, *Cell Tissue Res.* **2003**, *314*, 15.
[62] B Lilly, *Physiology* **2014**, *29*, 234.
[63] D. B. Cines, E. S. Pollak, C. A. Buck, J. Loscalzo, G. A. Zimmerman, R. P. McEver, J. S. Pober, T. M. Wick, B. A. Konkle, B. S. Schwartz, E. S. Barnathan, K. R. McCrae, B. A. Hug, A. M. Schmidt, D. M Stern, *Blood* **1998**, *91*, 3527.
[64] S. F. Rodrigues, D. N Granger, *Tissue Barriers* **2015**, *3*, e978720.
[65] C. Cheng, F. Helderman, D. Tempel, D. Segers, B. Hierck, R. Poelmann, A. van Tol, D. J. Duncker, D. Robbers-Visser, N. T. Ursem, R. van Haperen, J. J. Wentzel, F. Gijsen, A. F. van der Steen, R. de Crom, R Krams, *Atherosclerosis* **2007**, *195*, 225.
[66] S. SenBanerjee, Z. Lin, G. B. Atkins, D. M. Greif, R. M. Rao, A. Kumar, M. W. Feinberg, Z. Chen, D. I. Simon, F. W. Luscinskas, T. M. Michel, M. A. GimbroneJr., G. Garcia-Cardena, M. K Jain, *J. Exp. Med.* **2004**, *199*, 1305.
[67] G. B. Atkins, M. K Jain, *Circ. Res.* **2007**, *100*, 1686.
[68] L. Nayak, Z. Lin, M. K Jain, *Antioxid. Redox Signaling* **2011**, *15*, 1449.